

SYNTHESIS AND PROPERTIES OF INORGANIC COMPOUNDS

On the Structure and Dehydration of Hydrous Zirconia and Hafnia Xerogels

A. V. Kostrikin^a, F. M. Spiridonov^b, L. N. Komissarova^b, I. V. Lin'ko^c,
O. V. Kosenkova^a, and B. E. Zaitsev^c

^a Michurinsk State Pedagogical University, Michurinsk, Russia

^b Moscow State University, Moscow, 119991 Russia

^c Russian University of Peoples' Friendship, Moscow, Russia

e-mail: Radi1@rambler.ru

Received October 20, 2008

Abstract—Hydrous zirconia and hafnia xerogels of compositions $\text{ZrO}_2 \cdot 2.5\text{H}_2\text{O}$ and $\text{HfO}_2 \cdot 2.3\text{H}_2\text{O}$ are dehydrated in two steps upon heating. First, molecular water is mostly removed from the structures to form phases of compositions $\text{ZrO}_2 \cdot \text{H}_2\text{O}$ and $\text{HfO}_2 \cdot 0.5\text{H}_2\text{O}$. Second, polycondensation of OH groups occurs. Both processes are easier for $\text{ZrO}_2 \cdot 2.5\text{H}_2\text{O}$. Apart from these steps, the interaction of water molecules with zirconium–oxygen bridges was found to occur during dehydration of the zirconium compound. The composition of $\text{HfO}_2 \cdot 0.5\text{H}_2\text{O}$ should actually read as $\text{Hf}_4\text{O}_7(\text{H}_2\text{O})(\text{OH})_2$.

DOI: 10.1134/S0036023610060070

Hydrous dioxides of Group IV elements are used as catalysts for a number of chemical processes [1], as adsorbents for the recovery of platinum metals, mercury, and copper from complexing media [2], as well as fission and corrosion radionuclides from aqueous, and as liquid-metal cooling agents of reactors and in sewage decontamination [3].

Here we are concerned with the properties of hydrous zirconia and hafnia xerogels and their variations in response to thermal dehydration; we also generalize our results and compare them with the related literature.

EXPERIMENTAL

Hydrous zirconia is precipitated from acid solutions prepared by dissolving ZrCl_4 , $\text{Zr}(\text{SO}_4)_2$, $\text{ZrO}(\text{NO}_3)_2 \cdot n\text{H}_2\text{O}$, zirconyl chloride, and zirconyl sulfate using aqueous alkalis and ammonia or, very seldom, gaseous ammonia as precipitators. State-of-art processes for preparing hydrous zirconia are listed in Table.

When sulfuric acid derivatives and sodium or potassium are the starting reagents, the relevant cations are occluded by the precipitate and hardly removable by washing and subsequent drying [2, 4–14]. Processes employing nitric or perchloric acid derivatives are free of such drawbacks. Cl^- ions are readily solubilized from the precipitate [7], and it is far easier to wash the precipitate from these anions.

An interesting method is to prepare hydrous zirconia by hydrolysis of isopropoxide $\text{Zr}(\text{C}_3\text{H}_7\text{O})_4$ in aqueous nitric acid solution [8]. However, this method is

not widely used because of the high cost of the precursor zirconium compound. Noteworthy is the synthesis of hydrous zirconia $\text{ZrO}_2 \cdot n\text{H}_2\text{O}$ ($n = 0.3–0.1$) by means of $\text{ZrO}(\text{NO}_3)_2 \cdot n\text{H}_2\text{O}$ decomposition [15].

Hydrous hafnia with the degree of hydration depending on the precipitation parameters is recovered from solutions by analogy with zirconium compounds [16].

Having regard to the strengths and weaknesses of the prior art methods and the availability of precursors for hydrous zirconia and hafnia, we used the following procedure. A weighed portion of zirconium or hafnium tetrachloride (chemically pure grade) was dissolved in aqueous hydrochloric acid, which was prepared by diluting concentrated HCl (36 wt %) with distilled water to reach the ratio 1 : 1. Hydrous dioxides were precipitated from the resulting hot solution by concentrated aqueous ammonia. Precipitates were washed by decanting hot water until a negative test for chloride ion was obtained. As the washes gave the negative silver nitrate test for chloride ion, the sample was washed with hot water three or four times and then dried at 50°C to obtain a xerogel.

The thus-prepared $\text{MO}_2 \cdot n\text{H}_2\text{O}$ samples were studied by thermogravimetric analysis in combination with crystal-optical analysis, powder X-ray diffraction, and IR spectroscopy. Thermal curves were recorded on Q-1500D and OD-102 instruments in a dynamic mode (weight scale sensitivity: 100 mg; DTG sensitivity: 250 mV; DTA sensitivity: 250 mV; heating rate in air to 1000°C: 10 K/min; sample holder: an uncovered platinum crucible) and in a quasi-isothermal mode (heating in air to 1000°C; weight scale sensitivity:

100 mg; decomposition rate: 0.4 mg/min; sample holder: a covered conical-shaped platinum crucible). Sample sizes were varied within 200–300 mg.

Powder X-ray diffraction analysis was performed on DRON-3M, (CoK_α radiation, $\text{Fe}\beta$ filter, 0.1° 2θ scan steps, 5-s scan time per point).

Crystal-optical analysis was performed on an MIN-8 polarizing microscope using an IZh-1 immersion liquids kit.

IR spectra were recorded on Specord M 82 in the frequency range 4000–300 cm^{-1} as potassium bromide disks and Nujol mulls between potassium bromide platelets.

Specific surface areas of test samples were derived from thermal nitrogen adsorption measured on gas meter in a GKh setup. Reference specific surface areas were determined by measuring low-temperature krypton adsorption on a vacuum setup. The references used were silica gel KSS-3 (specific surface area: 600 m^2/g) and Silochrom SCh-3 (specific surface area: 110 m^2/g).

We find it necessary to mention that IR spectroscopy was used as a tool for verifying test samples for the absence of impurities in addition to powder X-ray diffraction and chemical analysis. Suspected impurities in the test samples were as follows: CO_3^{2-} , NH_4^+ , NO_3^- , and NO_2^- . The last two ions are formed as a result of transformations NH_4^+ ions under heating in air. Groups of light atoms (CO_3^{2-} , NO_3^- , and NO_2^-), which weakly interact with other atomic groups, give rise to strong (narrow and sharp) absorption bands in IR spectra with peaks at: CO_3^{2-} , ~879 cm^{-1} (v_2); NO_3^- , ~831 cm^{-1} (v_2); and NO_2^- , ~1244 cm^{-1} (v_3) [17]. Such bands were not observed in the IR spectra of the compounds described, which unequivocally signifies the absence of the relevant ions in the test samples. For NH_4^+ ion, the strongest band at 1400 cm^{-1} in the IR spectrum of NH_4Cl is recognized as the analytical band. Looking ahead, we mention that bands at similar frequencies appear in the IR spectra of the compounds recovered at 300, 700, 900, and 1000°C. However, it is highly problematic whether NH_4Cl is contained in our test samples at such temperatures. There are no reflections intrinsic to NH_4Cl in the X-ray diffraction patterns of these samples. Thus, the hydrous dioxide formula units suggested from gravimetric and thermogravimetric data are supported by powder X-ray diffraction and IR spectroscopy.

The recovered hydrous hafnia is a single phase as identified by crystal-optical analysis, and its composition is $\text{HfO}_2 \cdot 2.3\text{H}_2\text{O}$. The water content of the sample decreases under heating. The thermal decomposition of the compound in the dynamic mode starts at 50°C and is accompanied by a well-defined DTA endo-

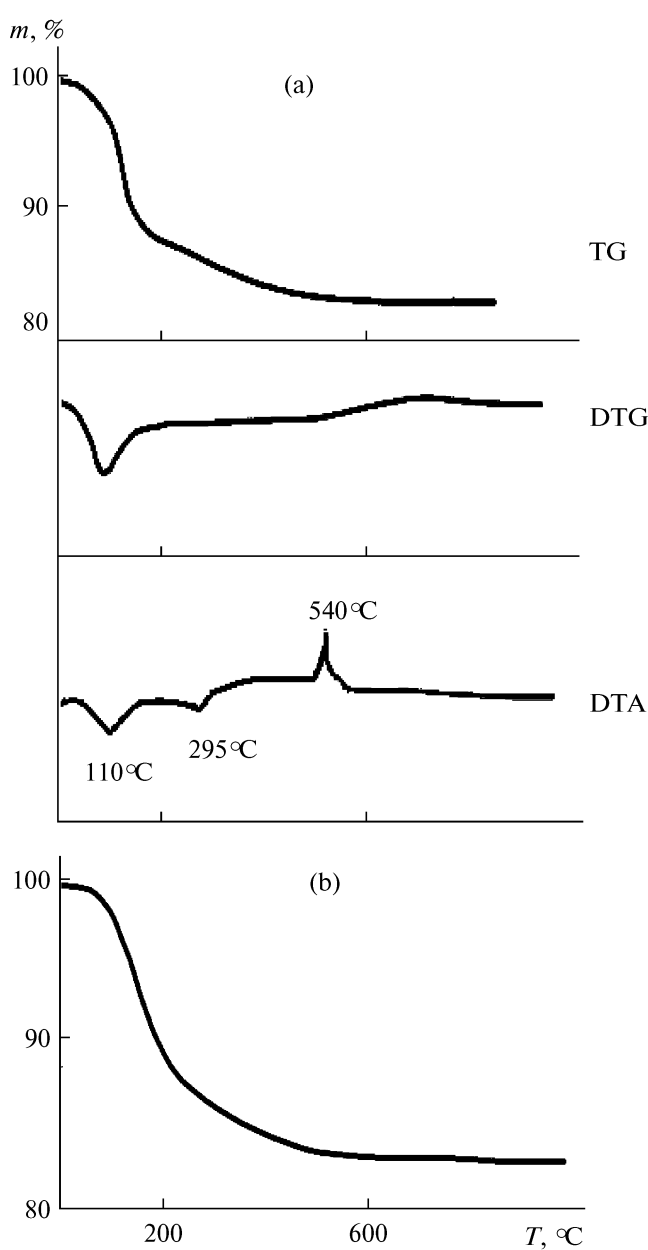


Fig. 1. Thermal curves for $\text{HfO}_2 \cdot 2.3\text{H}_2\text{O}$ hydrous hafnia samples recorded (a) in a dynamic heating mode and (b) in a quasi-isothermal mode.

therm (Fig. 1a) having a peak at about 110°C. In addition, a second weak endotherm appears at 295°C, being in part hidden by the next strong exotherm. A similar DTA curve (Fig. 1a) was earlier observed by Sakharov et al. [4], who found the DTA curve to ascend before entering the exotherm and who related this fact to “certain structural alterations” of amorphous dioxide in the “precrysalloization period.” The DTG weight-loss peak (Fig. 1a) is clearly skewed, and its skewness may appear an argument in favor of the two-step thermolysis scheme for hydrous hafnia. Thus, the features of the differential curves unequivo-

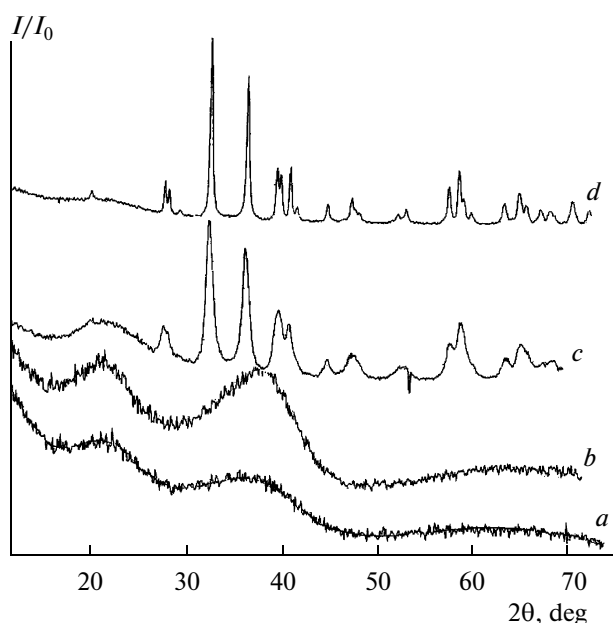


Fig. 2. X-ray diffraction patterns for $\text{HfO}_2 \cdot n\text{H}_2\text{O}$ samples recovered at (a) 50, (b) 300, (c) 400, and (d) 700°C.

cally indicate the two-step dehydration of the sample. As temperature increases further, the DTA curve features a strong narrow exotherm (with a peak at 540°C) associated with the crystallization of monoclinic hafnia [4, 18]. The positions of the first observed dehydration peak and the HfO_2 crystallization peak agree well with Kadoshnikova et al.'s data [19]; however, Kadoshnikova et al. [19] came to the conclusion of $\text{HfO}_2 \cdot n\text{H}_2\text{O}$ dehydration having one step. Poorly defined signatures of a second decomposition step are noticed only in comparatively large samples (weighing more than 200 mg). Smaller sample sizes do not allow these signatures to be detected for certain. Earlier [20], this also misled us to the conclusion of one-step $\text{HfO}_2 \cdot n\text{H}_2\text{O}$ thermolysis.

During the quasi-isothermal heating of $\text{HfO}_2 \cdot 2.3\text{H}_2\text{O}$ hydrous hafnia, the weight loss curve (Fig. 1b) does not feature horizontal or vertical segments. At 220°C, however, the curve changes its slope quite distinctly. This change is reproduced in TG curves recorded for various $\text{HfO}_2 \cdot 2.3\text{H}_2\text{O}$ sample sizes and corresponds to the elimination of 1.8 water molecules within 75–220°C. The remaining 0.5 water mole is removed within 220–520°C. The trend of the quasi-isothermal curve implies that the thermolysis of hydrous hafnia is a non-zero-order reaction (the weight loss associated with the elimination of molecular water is accompanied by OH-group polycondensation). Presumably, the range 75–220°C is where water molecules are eliminated and polycondensation has not great contribution. Within 220–520°C, polycondensation dominates. A phase of composition $\text{HfO}_2 \cdot 0.5\text{H}_2\text{O}$ was earlier found to form during thermolysis

[10]. In order to gain more data on the transformation of hydrous hafnia during dehydration, we prepared samples containing less water by heating the intact sample to constant weight at 120, 200, 300, 400, 700, and 1000°C. In choosing these heating temperatures for recovering the products of $\text{HfO}_2 \cdot 2.3\text{H}_2\text{O}$ thermolysis, we were guided by the results of our thermogravimetric investigations and the literature data on the transformations of hydrous hafnia. The relevant X-ray diffraction patterns are shown in Fig. 2, and specific surface areas are in Table 2.

The observed variations in specific surface area (Table 2) indicate that, most likely, the first thermolysis step involves the elimination of water mainly from individual particles of the xerogel, which is responsible for the increasing specific surface area of the sample. At the second step, weight loss is due to active dehydroxylation accompanied by particle coarsening and the associated decrease in the specific surface area.

The samples prepared at 50, 120, and 200°C are amorphous to X-rays. X-ray diffraction patterns of the samples prepared by heating hydrous hafnia above 400°C contain lines from monoclinic HfO_2 (Fig. 2) [4, 18, 19].

Thus, as hydrous hafnia is heated, water is eliminated in two steps according to the scheme below.



Weight loss calcd., %	12.9	3.6
Found, %	12.9	3.8

Hydrous zirconia xerogel has the following composition: $\text{ZrO}_2 \cdot 2.5\text{H}_2\text{O}$. Prozorovskaya et al. [10] prepared this xerogel by drying the precipitate at 20°C. This is an X-ray amorphous compound. However, its X-ray diffraction pattern (Fig. 3, curve *a*) contains broad reflections from interplanar spacings of 4.6795 and 2.9208 Å. Probably, this fact served as the basis for Nazarov [8] to infer that $\text{ZrO}_2 \cdot 2.5\text{H}_2\text{O}$ is a partially crystallized cubic phase.

$\text{ZrO}_2 \cdot 2.5\text{H}_2\text{O}$ under heating loses water rather intensely. Its thermal decomposition in a dynamic mode (Fig. 4a) occurs within 55–900°C and is accompanied by an endotherm (peaking at about 95°C) and then an exotherm (peaking at 395°C), the latter corresponding to the crystallization of tetragonal ZrO_2 ; its transition to the monoclinic phase occurs at a higher temperature [14]. The clear-cut skewed weight-loss DTG peak may signify the two-step thermolysis of $\text{ZrO}_2 \cdot 2.5\text{H}_2\text{O}$. Two dehydration steps were noted in [6, 21, 22].

The quasi-isothermal weight-loss curve (Fig. 4b) has a smooth run without horizontal arrests or vertical segments. At 145°C, however, the curve changes its slope. The break point corresponds to the elimination of 1.5 water moles. The remaining 1 water mole is eliminated within 145–900°C; the main loss is

Table 1. Syntheses of hydrous zirconia

Initial species	Precipitation process	Precipitation temperature	Other parameters	Source
ZrOCl ₂ ZrO(SO ₄)	Hydrolysis in 10% KOH or aq. NH ₃	Not specified	Not indicated	[4]
ZrOCl ₂	Precipit. by aq. ammonia	Not specified	Water washing and drying at various temp.	[10]
ZrOCl ₂	Precipit. by NaOH sln.	Ambient	Water washing, pulp refluxing, drying at 80 and 140°C	[11]
ZrCl ₄ ZrOCl ₂	Precipit. by aq. NH ₃ , gas. NH ₃	Ambient Ambient	pH control, water washing, drying at 120°C. Gel freezing followed by defrosting and water washing. Drying at 120°C	[7]
ZrO(SO ₄) Zr(SO ₄) ₂ ZrC ₁₄ ZrOCl ₂	Treat. of solids by KOH (10% and 20%) an NH ₃ aq. (1%)	Ambient	Not indicated	[5]
ZrO(NO ₃) ₂	Hydrolysis in NaOH sln.	Ambient	pH control, water washing by decantation with centrifuging	[2]
ZrO(NO ₃) ₂ ZrOCl ₂	Hydrolysis in aq. ammonia	Ambient	pH 10; repeated water wash., hydrothermal heating at 423–523 K	[12]
ZrC ₁₄	Precipit. by NaOH sln.	Not specified	pH 6; water wash., freez. at –12°C, again water wash.	[13]
ZrOCl ₂ · 8H ₂ O	Electrochemical precipit.	Ambient	Water washing and drying at room temperature to constant weight	[14]
ZrO(NO ₃) ₂	Precipit. by NaOH sln.	Not specified	pH 5.5, 7.0, 10.0; water washing by decantation, precipitate aging in NaOH and Na ₂ SO ₄ sln. (1 mol-equiv./L) at 80 and 96°C	[6]
ZrO(NO ₃) ₂	Precipit. by aq. ammonia	Ambient	pH 9; aging under mother sln., washing and drying at room temperature and 100°C	[9]
Zr(C ₃ H ₇ O) ₄	Hydrolysis by aq. HNO ₃	Ambient	Sol was investigated	[8]

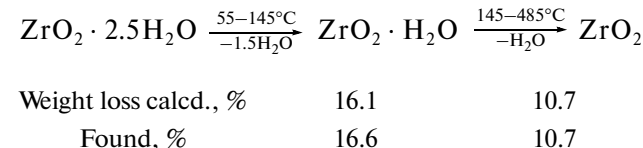
observed below 485°C. This run of the weight-loss curve indicates the non-zero order of the thermolysis reaction; that is, the weight loss associated with the elimination of molecular water is accompanied by the polycondensation of hydroxo groups. The pattern of the quasi-isothermal curve suggests that within 55–145°C the compound loses molecular water and polycondensation has not great contribution; within 145–900°C, polycondensation dominates.

To gain more dehydration data, ZrO₂ · 2.5H₂O was heated to 120, 200, 300, 700, and 900°C. These temperatures for recovering ZrO₂ · 2.5H₂O thermolysis products were chosen proceeding from the results of our thermogravimetric experiments and by analogy with the hafnium compound. As the heating temperature rises, the specific surface area of the sample decreases monotonically (Table 2). After a sample is

heated from 50 to 120°C, however, its specific surface area decreases by ~11 m²/g; heating from 120 to 200°C brings about a 77 m²/g decrease in specific surface area. Thus, we may infer the active dehydroxylation of the compound within 120–200°C, which leads to particle coarsening.

The samples recovered at 50, 120, and 200°C are X-ray amorphous (Fig. 3, curves *a*–*c*). The absence of crystalline phases was detected up to 400–450°C [23], in good agreement with our observed peak temperature (395°C) of the exotherm associated with zirconia crystallization. The lengthening heat treatment leads to the crystallization of the compound in the tetragonal phase and, then, a mixture of tetragonal and monoclinic ZrO₂ phases [9, 14, 22] (Fig. 3, curve *d*).

Thus, the heat-induced dehydration of the ZrO₂ · 2.5H₂O xerogel has two steps according to the scheme below.

**Table 2.** Specific surface areas (in m²/g) of hydrous zirconia and hafnia recovered at various temperatures

Temperature	50°C	120°C	200°C	700°C
ZrO ₂ · <i>n</i> H ₂ O	248.0	239.5	162.0	142.0
HfO ₂ · <i>n</i> H ₂ O	107.0	143.5	57.0	32.0

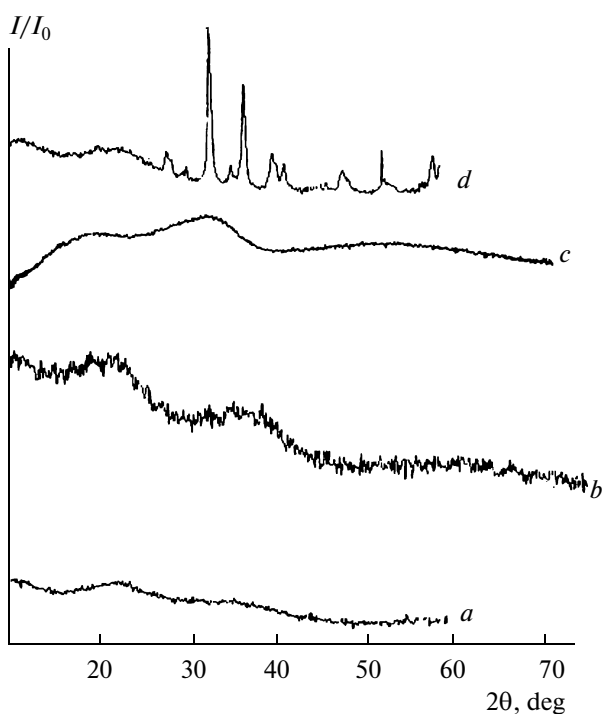


Fig. 3. X-ray diffraction patterns for $\text{ZrO}_2 \cdot n\text{H}_2\text{O}$ samples recovered at (a) 50, (b) 120, (c) 200, and (d) 700°C.

In view of the detailed consideration of the properties of hafnium hydroxo salts by Ivanov-Emin et al. [24], the IR spectroscopic data for $\text{HfO}_2 \cdot 2.3\text{H}_2\text{O}$ are interpreted with high consistency. This allowed us to study the properties of hydrous hafnia in a detailed way and, then, interpret experimental data on zirconium compounds by analogy.

Figure 5 shows the IR spectra of an $\text{HfO}_2 \cdot 2.3\text{H}_2\text{O}$ sample and the products of its thermolysis recovered at various temperatures. Assignment was performed on the basis of related literature [24–27] and our experimental data (Table 3). Apart from this, we obtained IR spectra from anhydrous hafnia, potassium hexahydroxohafnate, and potassium oxohydroxohafnates (as Nujol mulls in sodium chloride platelets). Comparative analysis allowed the more consistent assignment.

$\text{HfO}_2 \cdot 2.3\text{H}_2\text{O}$ is a compound built of the following atomic groups (Table 3): OH groups (either unbound or bound by strong hydrogen bonds), H_2O molecules, $\text{Hf}=\text{O}-\text{H}$ terminal groups, and $\text{Hf}=\text{O}(\text{H})-\text{Hf}$ and $\text{Hf}=\text{O}-\text{Hf}$ bridging groups, these groups appearing in the IR spectrum as individual or composite absorption bands.

As temperature rises, the absorption bands associated with the vibrations of hydroxo groups and water molecules dramatically weaken until complete disappearance (Table 3). At 120°C, the $\delta(\text{H}_2\text{O})$ band is split to high-frequency and low-frequency components. At 200°C, the low-frequency component disappears and the high-frequency shift of the other component peak

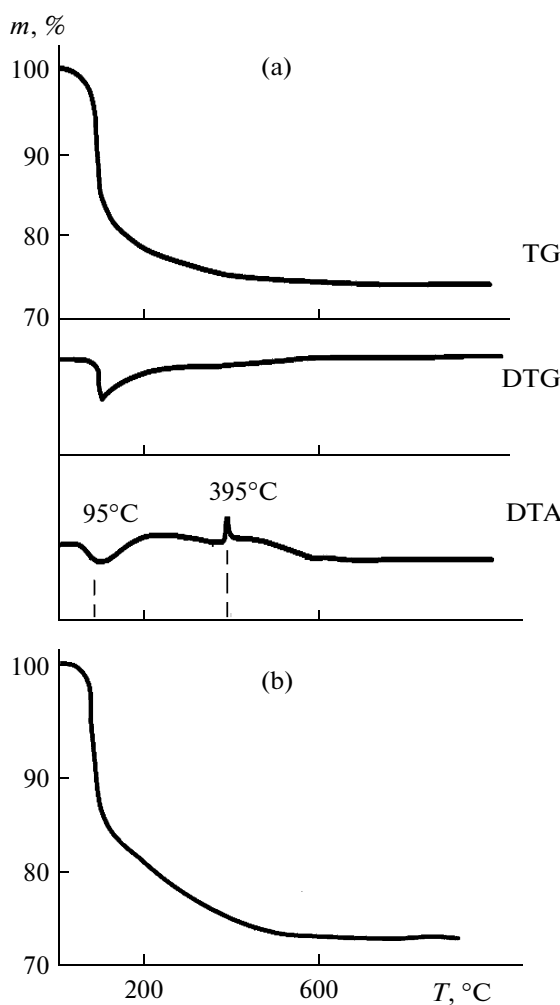


Fig. 4. Thermal curves for hydrous zirconia $\text{ZrO}_2 \cdot 2.5\text{H}_2\text{O}$ samples recorded (a) in a dynamic heating mode and (b) in a quasi-isothermal mode.

is enhanced. This implies the elimination of relatively weakly bound water molecules from $\text{HfO}_2 \cdot 2.3\text{H}_2\text{O}$ upon heating to 200°C and the enhancement of interactions of the remaining water molecules with the structural elements of the compound.

The IR spectrum of the thermolysis product recovered at 1000°C and exposed in air for several hours features absorption bands associated with hydroxo groups and water molecules. In all probability, the occurrence of water vapor in the laboratory atmosphere leads to rehydration upon cooling the instrument after experiments. The comparison of the intensity of the $\delta(\text{H}_2\text{O})$ absorption band with the $\delta(\text{Hf}=\text{O}(\text{H})-\text{Hf})$ and $\delta(\text{HfOH})$ bands in the IR spectrum of the thermolysis product and a similar intercomparison with the IR spectrum of $\text{HfO}_2 \cdot 2.3\text{H}_2\text{O}$, implies the low rehydration rates of $\text{Hf}=\text{O}-\text{Hf}$ olic bonds.

The assignment of $\text{ZrO}_2 \cdot 2.5\text{H}_2\text{O}$ absorption bands in the IR spectrum (Table 4) was based on (a) the

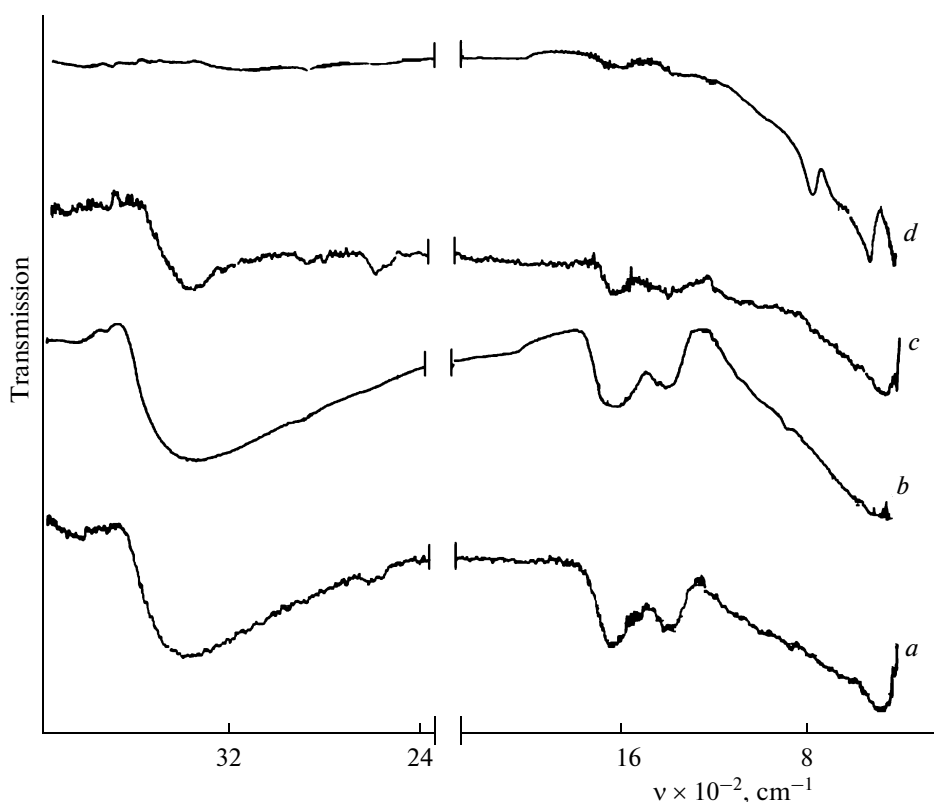


Fig. 5. IR spectra of $\text{HfO}_2 \cdot n\text{H}_2\text{O}$ samples recovered at (a) 50, (b) 120, (c) 200, and (d) 700°C.

results of thermogravimetric experiments, (b) related literature [24, 26, 28–32], and (c) by analogy with the IR spectra of $\text{HfO}_2 \cdot 2.3\text{H}_2\text{O}$ and its thermolysis products. The $\text{ZrO}_2 \cdot 2.5\text{H}_2\text{O}$ spectrum features several absorption bands signifying the presence of OH groups (unbound or bound in strong hydrogen bonds), H_2O molecules, Zr—O—H terminal groups and Zr—O(H)—Zr and Zr—O—Zr bridging groups.

Notably, the absorption peak at 1575 cm^{-1} is due to the bending vibrations $\delta(\text{H}_2\text{O})$ of water encapsulated in mesopores in the form of vapor (Table 4). Trens [21] detected this type of water in a $\text{ZrO}_2 \cdot n\text{H}_2\text{O}$ sample.

Once the heating temperature is raised to 200°C, new absorption bands appear in a $\text{ZrO}_2 \cdot 2.5\text{H}_2\text{O}$ sample (Table 4, Fig. 6). The intensities of these newly resolved bands (peaks at 1529 and 1490 cm^{-1}) decrease dramatically in response to rising temperature. Thus, these bands are associated with the vibrations of hydroxyl-containing groups, which are most likely Zr—O(H)—Zr. The assignment of these absorption bands to the vibrations of bridging bonds may be justified by the following reasons. Compounds with a high E—OH bond covalence feature the bands of $\delta(\text{EOH})$ vibrations in a high-frequency region (1300 – 1400 cm^{-1} [29, 33]); in the IR spectrum of gaseous methanol, for example, the $\delta(\text{COH})$ band appears at 1340 cm^{-1} [34]. Interaction enhancement as a result of, for example, the bidentate binding of an OH group will cause this band

to shift to high frequencies. For example, in the spectrum of the $\text{SnO}_2 \cdot 1.75\text{H}_2\text{O}$ analogue, the absorption band responsible for the $\delta(\text{Sn—O(H)—Sn})$ vibrations appears at 1406 cm^{-1} , and the $\delta(\text{Sn—OH})$ mode appears at 1270 – 1070 cm^{-1} [35]. Therefore, the absorption bands in the IR spectra of $\text{ZrO}_2 \cdot 2.5\text{H}_2\text{O}$ and its thermolysis products with peaks in the region of 1530 – 1330 cm^{-1} , which change their intensity to disappear upon heating, can fairly arise from the vibrations of bridging bonds ($\delta(\text{Zr—O(H)—Zr})$ mode).

RESULTS AND DISCUSSION

Hydrous zirconia is prepared by hydrolyzing oxochloride or another zirconium compound, but zirconium oxochloride ZrOCl_2 is always involved in the conversion chain.

There is abundant literature on the hydrolysis of chloride compounds of zirconium, and diversified investigation tools were used, namely, diffusion [36–39], dialysis [40], potentiometry [39, 41], cryoscopy [39, 41], spectrophotometry [42], and partition [43]. As to the structure of hydrous zirconia, a reasonable assumption is that the structure of the initial compound (in the case, zirconium oxochloride) dictates the structure of the precipitated product [4]. X-ray crystallography [44] shows that hydrous zirconium oxochloride $\text{ZrOCl}_2 \cdot 8\text{H}_2\text{O}$ is built of tetrameric cyclic

Table 3. Absorption peaks (in cm^{-1}), their relative intensities, and assignment in the IR spectra of oxygen-and-hydroxyl-containing hafnium compounds recovered at various temperatures

HfO ₂ · 2.3H ₂ O and its thermolysis products					HfO ₂ comp.	K ₂ Hf(OH) ₆		K ₂ Hf ₂ O ₃ (OH) ₅	Assignment	
50°C	120°C	200°C	700°C	1000°C	25°C	25°C	220°C	250°C		
3748 w	3748 w	3526 sh 3403 m 3404 s	3470 w 3411 w		3721 m 3661 w	3734 m	3729 w 3593 sh		v(OH)	
2979 s	2924 sh	3363 s 3366 m 3280 m 3159 m 2920 m	3203 w 2916 w		3210 s	3434 sh 3305 s 3154 s	3300 w 3200 s			
1603 s	1616 sh 1576 s	1629 m	1583 w	1610 w	Not appear.	Not appear.	Not appear.	Not appear.	δ(H ₂ O)	
1391 m	1460 m	1480 w	1401 w		Nujol bands	Nujol bands	Nujol bands	Nujol bands		
1358 s	1364 s	1392 m	1364 w	1365 w					δ(Hf—O(H)—Hf)	
1112 w 1063 m	1056 sh	1146 sh 1088 m 1002 m 963 sh	967 sh	967 w	979 sh			1055 sh		
967 sh	959 sh	842 s	846 sh	856 m		925 s 885 sh 819 sh 779 s	950 s 897 m 850 m	995 s 885 w 844 sh 788 s	δ(HfOH)	2v(HfO)
767 s	785 sh	778 sh	766 s	769 m	776 m 733 m					
652 sh	664 sh	663 sh 613 s	661 sh 640 sh	661 sh	Intens. absorp- tion			625 w	v(HfO)	
597 sh 464 s	547 sh 468 s	550 sh 480 s	524 s	517 s		473 s 433 sh	460 s	617 w 560 w 483 s		

fragments $[\text{Zr}_4(\text{OH})_8]^{8+}$. These fragments also contain 16 water molecules (four molecules per zirconium atom). When alkali is added, some water molecules, clearly, enter OH groups to form $[\text{Zr}_4(\text{OH})_8^{\text{b}}(\text{OH})_4^{\text{t}} \cdot 12\text{H}_2\text{O}]^{4+}$, fragments, where OH^b are bridging hydroxo groups and OH^t are terminal hydroxo groups [39, 45]. The process ends with the formation of $[\text{Zr}_4(\text{OH})_8^{\text{b}}(\text{OH})_8^{\text{t}} \cdot 8\text{H}_2\text{O}]^0$ uncharged fragments. These fragments are linked by hydrogen and Zr—O(H)—Zr bridging bonds to form grains with sizes from 3 to 64 nm [8, 46]. Sometimes, they contain up to 70 tetramers per grain [8]. This structure of the polymer in zirconium oxochloride solutions is responsible for its increased viscosity [39]. Bridging bonds between tetramers are less strong (here, steric factors are important) and are more easily destroyed by acids or alkalis or as the solution temperature increases. This explains the existence of species with strongly diversified molecular weights (from 800 to 2600 [36] to 5400–7000 a.m.u. [46]) in solutions of various compositions. The same is responsible for a varied degree

of polymerization, which always exceeds four [40, 41] and depends on the solution acidity.

Probably, hydrous hafnia HfO₂ · 2.3H₂O is also built of tetrameric hafnium—oxygen—hydroxide fragments, like those of which hydrous zirconia is built [11]. It contains Hf—O(H)—Hf and Hf—OH atomic groups and water molecules. These hydroxyl-containing groups and water molecules take part in hydrogen bonding between structural elements. A particular indication of this hydrous hafnia structure is the formation of a compound of the Na₂Hf₄O₉ · 5H₂O tetrameric anion in the low-alkali region (less than 3.18 mol/L) in the Na₂O—HfO₂aq—H₂O system [47]. The existence of Hf₄(OH)₈⁸⁺ tetrameric cation was noted in perchloric acid solutions when hafnium concentrations were less than 10⁻³ mol/L [48].

While being dried, the hydrolysis products experience the following transformations: sol → gel → xerogel. These transformations are accompanied by a decrease in the number of water molecules in polymeric fragments. ZrO₂ · 2.5H₂O and HfO₂ · 2.5H₂O are formed in this way.

Table 4. Absorption peaks (in cm^{-1}), their relative intensities, and assignment in the IR spectra of $\text{ZrO}_2 \cdot n\text{H}_2\text{O}$ samples recovered at various temperatures

$\text{ZrO}_2 \cdot 2.5\text{H}_2\text{O}$ and its thermolysis products					Assignment
50°C	120°C	200°C	300°C	900°C	
3542 s		3545 m	3592 w	3588 w 3534 w	
3475 s	3492 s	3463 m			
	3428 s	3417 m	3448 w	3417 sh	
	3411 s	3381 m			
3337 s	3348 s	3344 m	3341 w	3367 w	
	3307 s	3292 m			
3261 s	3240 s	3237 m	3245 w	3277 w	$\nu(\text{OH})$
	3203 sh	3188 m			
	3153 s	3146 m	3155 w		
3110 s	3100 s	3099 m	3076 w		
	3054 sh	3040 m			
3017 s	3004 sh	3014 m			
		2945 m			
2863 s	2849 s	2832 m			
	2681 s	2720 m			
1599 s	1598 s	1622 s	1648 w	1631 w	$\delta(\text{H}_2\text{O})$
		1596 s	1623 w		
1575 s			1571 s		$\delta(\text{H}_2\text{O})$ in pores
1524 s	1506 s	1529 m	1532 w		
		1490 m	1455 sh	1406 sh	
1357 s	1354 s	1362 s	1398 sh	1350 sh	$\delta(\text{Zr}-\text{O}(\text{H})-\text{Zr})$
1333 sh			1326 sh		
1169 sh	1188 w	1269 w			
1059 sh	1057 sh	1197 w	1105 w		
983 s	970 s	1061 sh	1034 w		
938 s	942 s	976 s		995 w	$\delta(\text{ZrOH})$
847 s	853 s	946 s	938 w		
		848 s			
703 s	774 sh	775 s	785 sh		
661 s	704 sh	721 s	737 sh	743 s	
	650 sh	692 s	665 s	681 sh	
592 s			634 sh		
562 s		563 s	606 s	583 s	$\nu(\text{ZrO})$
515 s	525 s		515 s	509 s	
473 s	478 s	489 s	482 s		
439 s		424 s		424 s	
404 s	404 s				
372 s	372 s	346 s			

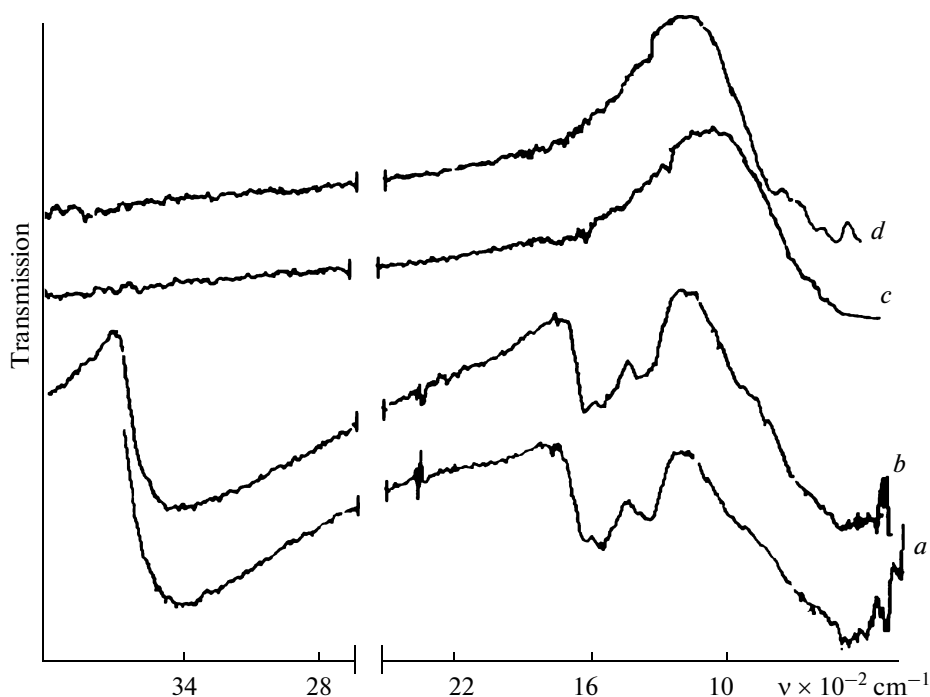


Fig. 6. IR spectra of $\text{ZrO}_2 \cdot n\text{H}_2\text{O}$ samples recovered at (a) 50, (b) 120, (c) 200, and (d) 900°C.

Xerogel dehydration occurs in two steps. From $\text{ZrO}_2 \cdot 2.5\text{H}_2\text{O}$, unlike from hydrous hafnia, water is eliminated even at the first thermolysis step as a result of the polycondensation of hydroxo groups being rather intense. The second thermolysis step is almost completely due to the polycondensation of hydroxo groups. $\text{HfO}_2 \cdot 2.3\text{H}_2\text{O}$ has the following noteworthy dehydration feature: water molecules almost do not interact with hafnium–oxygen bridges under heating. Here, we will mention the results of the ^1H NMR investigation of $\text{HfO}_2 \cdot 2.3\text{H}_2\text{O}$ and $\text{ZrO}_2 \cdot 2.5\text{H}_2\text{O}$ performed by Prozorovskaya et al. [10]. They discovered that the number of hydroxo groups per mole of hafnium atoms in the structure of hydrous hafnia is constant within 20–125°C.

Having regard to the results of this work and the related literature, we may infer for hydrous hafnia of composition $\text{HfO}_2 \cdot 0.5\text{H}_2\text{O}$ that its valid formula unit is $\text{Hf}_4\text{O}_7(\text{OH})_2(\text{H}_2\text{O})$; this compound is structurally built of tetrameric cyclic fragments. For the zirconium compound, polycondensation of hydroxo groups is more intense. This difference arises from different interactions of the metal cation with hydroxo groups. In the hafnium compound, the M–OH bond is stronger. This is supported by comparison of E–F bond energy values, where E = Sn, Zr, or Hf. Such analogies are not quite adequate, because OH⁻ and F⁻ are iso-electronic species, have identical weights, and are similar in size. The bond energy (in kJ/mol) [49] is 646 for Hf–F, 616 for Zr–F, and 473 for Sn–F. The interactions of water molecules with E–O–E element–oxy-

gen bridges are enhanced in the same order, namely, in the Hf → Zr → Sn series of compounds. Rehydration is responsible for variations in zero-charge point pHs (pH_{zcp}) of hydrous dioxide surfaces found from the results of potentiometric titration [50]. As the drying temperature of hydrous hafnia increases, the pH_{zcp} increases monotonically, too; for $\text{ZrO}_2 \cdot n\text{H}_2\text{O}$ and $\text{SnO}_2 \cdot n\text{H}_2\text{O}$, in contrast, these values shift down. The interactions of water molecules with oxygen bridges in the structure of the last two hydrous oxides increase the amount of hydroxo groups on particle surfaces, and this in turn decreases pH_{zcp} .

REFERENCES

1. T. Hattori, S. Athoh, T. Tagava, and J. Murakami, *Preparation of Catalysts IV* (Elsevier, Amsterdam, 1987), p. 113.
2. S. I. Pechenyuk, Izv. Akad. Nauk, Ser. Khim., No. 2, 229 (1999).
3. Yu. I. Sukharev, *Synthesis and Applications of Specific Oxohydrate Sorbents* (Energoatomizdat, Moscow, 1987) [in Russian].
4. V. V. Sakharov, L. M. Zaitsev, V. N. Zabelin, and I. A. Apraksin, Zh. Neorg. Khim. **17** (9), 2392 (1972).
5. L. M. Zaitsev, V. N. Zabelin, V. V. Sakharov, et al., Zh. Neorg. Khim. **17** (1), 60 (1972).
6. S. I. Pechenyuk, N. L. Mikhailova, and L. F. Kuz'mich, Zh. Neorg. Khim. **48** (9), 1420 (2003) [Russ. J. Inorg. Chem. **48** (9), 1286 (2003)].

7. H. T. Rayten, in *Physical and Chemical Aspects of Adsorbents and Catalysts*, Ed. by B. Linsen (Academic Press, London, 1970; Mir, Moscow, 1973).
8. V. V. Nazarov, Extended Abstract of Doctoral Dissertation in Chemistry (Moscow, 1995).
9. N. N. Oleinikov, G. P. Murav'eva, and I. V. Pentin, *Zh. Neorg. Khim.* **47** (5), 754 (2002) [Russ. J. Inorg. Chem. **47** (5), 666 (2002)].
10. Z. N. Prozorovskaya, V. F. Chuvaev, L. N. Komissarova, et al., *Zh. Neorg. Khim.* **16** (6), 1524 (1972).
11. N. F. Savenko, I. A. Sheka, I. V. Matyash, and A. I. Kalinichenko, *Ukr. Khim. Zh.* **39** (1), 79 (1973).
12. Yu. V. Kolen'ko, A. A. Burukhin, B. R. Churagulov, et al., *Zh. Neorg. Khim.* **47** (11), 1755 (2002) [Russ. J. Inorg. Chem. **47** (11), 1609 (2002)].
13. V. A. Tarnopol'skii, A. D. Aliev, S. A. Novikova, and A. I. Kalinichenko, *Zh. Neorg. Khim.* **47** (11), 1763 (2002) [Russ. J. Inorg. Chem. **47** (11), 1616 (2002)].
14. L. G. Karakchiev, E. G. Avakumov, O. B. Vinokurova, et al., *Zh. Neorg. Khim.* **48** (10), 1589 (2003) [Russ. J. Inorg. Chem. **48** (10), 1447 (2003)].
15. A. S. Sinitskii, V. A. Ketsko, I. V. Pentin, et al., *Zh. Neorg. Khim.* **48** (3), 484 (2003) [Russ. J. Inorg. Chem. **48** (3), 406 (2003)].
16. F. Cotton and G. Wilkinson, *Advanced Inorganic Chemistry* (Wiley, New York, 1966; Mir, Moscow, 1969).
17. K. Nakamoto, *Infrared and Raman Spectra of Inorganic and Coordination Compounds* (Wiley, New York, 1986; Mir, Moscow, 1991).
18. ASTM, card no. 6-318.
19. N. V. Kadoshnikova, G. V. Rodicheva, V. P. Orlovskii, and I. V. Tananaev, *Zh. Neorg. Khim.* **35** (2), 326 (1990).
20. A. V. Kostrikin, I. G. Gorichev, F. M. Spiridonov, et al., *Zh. Neorg. Khim.* **45** (11), 1932 (2000) [Russ. J. Inorg. Chem. **45** (11), 1786 (2000)].
21. P. Trens, M. J. Hudson, and R. Denoyel, *J. Mater. Chem.* **8**, 2147 (1998).
22. I. A. Stenina, E. Yu. Voropayeva, T. R. Brueva, et al., *Zh. Neorg. Khim.* **53** (6), 912 (2008) [Russ. J. Inorg. Chem. **53** (6), 842 (2008)].
23. L. M. Zaitsev and T. N. Shubina, *Zh. Neorg. Khim.* **11** (8), 1592 (1966).
24. B. N. Ivanov-Emin, A. V. Kostrikin, F. M. Spiridonov, et al., *Zh. Neorg. Khim.* **41** (11), 1812 (1996) [Russ. J. Inorg. Chem. **41** (11), 1718 (1996)].
25. B. E. Zaitsev, *The Spectroscopy Coordination Compounds* (Izd-vo Universiteta druzhby narodov, Moscow, 1991) [in Russian].
26. G. V. Yakhnevich, *Infrared Spectroscopy of Water* (Nauka, Moscow, 1973) [in Russian].
27. V. N. Makatun, *The Chemistry of Inorganic Hydrates* (Nauka i Tekhnika, Minsk, 1985) [in Russian].
28. *The Hydrogen Bond*, Ed. by N. D. Sokolov (Nauka, Moscow, 1981) [in Russian].
29. M. Maltesse and W. J. Orville-Thomas, *J. Inorg. Nucl. Chem.* **29**, 2533 (1967).
30. J. Deabriges and R. Rohmer, *Bull. Soc. Chim. Fr.*, No. 1, 1 (1967).
31. A. V. Kostrikin, Candidate's Dissertation in Chemistry (MGPI im. V.I. Lenina, Moscow, 1988).
32. R. V. Kuznetsova, Candidate's Dissertation in Chemistry (RUDN, Moscow, 2000).
33. L. P. Petrishcheva, Candidate's Dissertation in Chemistry (MITKhT im. M.V. Lomonosova, Moscow, 1985).
34. A. V. Stuart and G. B. B. Sutherland, *J. Phys. Radium* **15**, 321 (1954).
35. A. V. Kostrikin, F. M. Spiridonov, I. V. Lin'ko, et al., *Zh. Neorg. Khim.* **52** (7), 1176 (2007) [Russ. J. Inorg. Chem. **52** (7), 1098 (2007)].
36. G. Jander and K. F. Jahr, *Koll. Beih.* **43**, 295 (1936).
37. B. A. Lister and L. A. McDonald, *J. Chem. Soc.*, 4315 (1952).
38. V. M. Kolikov, *Zh. Prikl. Khim.* **34**, 248 (1961).
39. A. N. Ermakov, I. N. Marov, and V. K. Belyaeva, *Zh. Neorg. Khim.* **8** (7), 1623 (1963).
40. A. K. Babko and G. I. Gridchina, *Zh. Neorg. Khim.* **6** (6), 1336 (1961).
41. M. Adolf and W. Pauli, *Koll. Z.* **B29**, 173 (1921).
42. A. J. Zielen and R. E. Connick, *J. Am. Chem. Soc.* **78**, 5785 (1956).
43. R. E. Connick and W. H. Reas, *J. Am. Chem. Soc.* **73**, 1171 (1951).
44. A. Clearfield and P. A. Vaughan, *Acta Crystallogr.* **9**, 555 (1956).
45. R. J. H. Clark, D. C. Bradley, and P. Thornton, *The Chemistry of Titanium, Zirconium and Hafnium* (Pergamon, Oxford/New York/Toronto/Sydney/Paris/Braunschweig, 1975), p. 449.
46. L. G. Karakchiev and N. Z. Lyakhov, *Zh. Neorg. Khim.* **40** (2), 238 (1995).
47. B. N. Ivanov-Emin, A. V. Kostrikin, F. M. Spiridonov, and A. I. Ezhov, *Zh. Neorg. Khim.* **39** (5), 777 (1994).
48. V. M. Peshkova and An Pen, *Zh. Neorg. Khim.* **7** (9), 2110 (1962).
49. S. S. Batsanov, *Structural Chemistry. Facts and Correlations* (Dialog-MGU, Moscow, 2000) [in Russian].
50. A. V. Kostrikin, I. G. Gorichev, I. V. Lin'ko, et al., *Zh. Neorg. Khim.* **50** (3), 389 (2005) [Russ. J. Inorg. Chem. **50** (3), 339 (2005)].